

Research Paper

Keratin17 Promotes Tumor Growth and is Associated with Poor Prognosis in Gastric Cancer

Hao Hu^{1,2}, Dan-hua Xu¹, Xiao-xu Huang², Chun-chao Zhu¹, Jia Xu¹, Zi-zhen Zhang¹✉, Gang Zhao¹✉

1. Department of Gastrointestinal Surgery, Ren Ji Hospital, Shanghai Jiao Tong University School of Medicine, Shanghai 200127, China.
2. Department of Gastrointestinal Surgery, Yijishan Hospital, Wannan Medical College, Wuhu, 241001, China

Hao Hu and Dan-hua Xu contributed equally to this article.

✉ Corresponding authors: Gang Zhao, PHD, Department of General Surgery, Ren Ji Hospital, School Medicine, Shanghai Jiao Tong University, No. 1630, Dongfang Road, Shanghai 200127, China. Tel: 86-021-68383711; Fax: +8602168383731; E-mail: zhaogang74313@aliyun.com and Zi-zhen Zhang, PHD, Department of General Surgery, Ren Ji Hospital, School of Medicine, Shanghai Jiao Tong University, No. 1630, Dongfang Road, Shanghai 200127, China. Tel: +8602168383731; E-mail: zzzhang16@hotmail.com

© Ivyspring International Publisher. This is an open access article distributed under the terms of the Creative Commons Attribution (CC BY-NC) license (<https://creativecommons.org/licenses/by-nc/4.0/>). See <http://ivyspring.com/terms> for full terms and conditions.

Received: 2017.02.27; Accepted: 2017.10.24; Published: 2018.01.01

Abstract

Krt17 is a 48kDa protein member of keratin family. Previous literatures have demonstrated Krt17 may play a promotive role in the progression of various malignancies. However, the exact function of Krt17 in the carcinogenesis and the progression of gastric cancer (GC) remains unknown. In the present study, the expression of Krt17 in 20 fresh GC and matched normal tissues were detected and Krt17 was found to be significantly increased in GC tissues compared to normal tissues. And then the immunohistochemistry was performed to investigate the Krt17 expression in 569 GC tissue specimens, we found that the expression of Krt17 was remarkably positively correlated with the tumor size ($P < 0.01$), depth of invasion (T) ($P < 0.001$), lymph node metastasis (N) ($P < 0.001$), tumor node metastasis (TNM) stage ($P < 0.001$) and vascular invasion ($P < 0.05$). High expression of Krt17 predicted a poor prognosis of GC patients. In addition, we showed silencing of Krt17 inhibited GC cell proliferation, migration and invasion, and induced cell apoptosis by altering Bcl2 family protein expression and cleaved caspase3 upregulation. Moreover, silencing of Krt17 led to cell cycle arrest at G1/S stage by decreasing cyclin E1 and cyclin D expression. In conclusion, our findings revealed Krt17 can be used as a novel predictive biomarker, thus providing a novel therapeutic target for GC patients.

Key words: Krt17, GC, Prognosis, Proliferation, Migration and invasion, Apoptosis, Cell cycle

Introduction

Gastric cancer (GC) is the fourth most commonly diagnosed malignancy and the second leading cause of cancer-related mortality worldwide [1, 2]. Existing therapeutic methods, such as surgery or chemotherapy, are not satisfactory because of the advanced stage of the disease, and the fact that it is often accompanied by malignant proliferation, extensive invasion, and lymphatic metastasis when diagnosed [3, 4]. Therefore, it is essential to discover novel potential molecular markers that are more effective for treating patients with GC.

Keratins (Krts), including 28 type I and 26 type II keratins, are the intermediate filament forming

proteins of epithelial cells, and constitute an indispensable part of cytoskeleton [5, 6]. Loss or mutations in keratins that cause or predispose to human diseases can lead to increased sensitivity to apoptosis and regulation of innate immunity [7]. In previous decades, the role of the keratin family in human cancers has been widely studied, and has caused great concern. For example, Krt14 was found to serve a pivotal role in the regeneration and tumorigenesis of bladder cancer [8]. A recent study reported that increased Krt7 expression might mediate lncRNA Krt7-AS induced GC progression [9]. Krt17 was originally discovered as a major constituent

of basal cell skin carcinoma [10], and is a member of the type I acidic epithelial keratin family [11]. In normal human epithelia, Krt17 expression is identified in various glands, including the respiratory epithelium and urothelium, and Krt17 is regarded as a basal/myoepithelial cell keratin [12, 13]. In addition to its scaffolding function, the expression of Krt17 is closely related to several types of cancer, and it acts as an oncoprotein by controlling the ability of p27 (KIP1) to influence cervical cancer pathogenesis [14]. Existing literatures report Krt17 is involved in the tumorigenesis of skin tumors [15], breast cancer [16], esophageal squamous cell carcinoma [17], colorectal carcinoma [18], pancreatic ductal adenocarcinoma [19], amongst others. However, the role of Krt17 in the development of GC is yet to be elucidated.

In our study, we analysed the expression of Krt17 in GC tissues and the corresponding normal tissues. The clinicopathological significance was determined by examining the expression of Krt17 using immunohistochemical staining in large samples of gastric tissue. In addition, we further elucidated the biological impact of Krt17 on GC cell lines.

Material and methods

In silico analysis using the The Cancer Genome Atlas (TCGA) and ONCOMINE databases.

To investigate the expression pattern of Krt17 in GC, we used two datasets (<https://tcga-data.nci.nih.gov/>) (www.oncomine.com/). Data was collected and analysed using R 3.0.2 software. Krt17 gene expression in GC tissues and normal tissues were compared according to the standard calculation method as previously described. [20].

Clinical tissue samples

Tissue microarrays consisting of 569 GC samples were all obtained from the Renji Hospital (Shanghai, China) between January 2005 and December 2011. An additional 20 freshly-frozen GC tissues and matched non-cancerous tissues were also obtained from patients who underwent surgical resection at the Renji Hospital. None of these patients had received radiotherapy, chemotherapy, hormone therapy or other related anti-tumour therapies before surgery. None of these patients had additional cancers diagnoses. Postoperative adjuvant therapies were performed, according to standard schedules and doses. Patients were followed-up every 6 months by telephone or at outpatient clinic till July, 2015 or dead. Patients' death information was obtained from their family. The follow-up time was calculated from the date of surgery to the date of death, or the last known follow-up. All samples were collected with

participants' written informed consent, and the experiments were approved by the local ethics committee of the Renji Hospital, Shanghai Jiaotong University School of Medicine.

Tissue microarrays construction

Tissue microarrays were constructed by Shanghai Zhuoli Biological Technology Co. Ltd. (Shanghai, China). Tissue paraffin blocks of Krt17 samples from 569 cases were stained with hematoxylin-eosin to confirm the diagnoses and marked at fixed points with most typical histological characteristics under a microscope. Two 1.5-mm cores per donor block were transferred into a recipient block tissue microarray, and each dot array contained fewer than 160 dots. Three-micron-thick sections were cut from the recipient block and transferred to glass slides with an adhesive tape transfer system for ultraviolet cross-linkage.

Immunohistochemistry (IHC) staining

IHC staining was performed according to a previously described procedure [21]. Krt17 rabbit polyclonal antibody (1:200, Proteintech, USA), PCNA (1:1000, Abcam, USA), cleaved caspase-3 (1:1000, CST, USA) were used. All sections were observed and imaged using a microscope (Axio Imager: Carl Zeiss). Scoring was conducted according to the ratio of positively stained cells (0 = negative, 1 = 1-25% of cells, 2 = 26-50% of cells, 3 = 51-75% of cells and 4 = 76-100% of cells were stained) and staining intensity (no staining scored 0, weakly staining scored 1, moderately staining scored 2 and strongly staining scored 3). The final score of Krt17 was designated using the proportion of positive cell score × staining intensity score as follows: “-” for a score of 0-2, “+” for a score of 3-5, “++” for a score of 6-9 and “+++” for a score of > 9. Low expression was defined as a total score < 6 and high expression as a total score ≥ 6. These scores were determined in a blinded manner by two senior pathologists and mean percentage values of two scores were taken.

Cell culture

GC cell lines SGC-7901, MKN45, MGC-803, BGC823, and HGC-27 were gifted from the Shanghai Cancer Institute, Renji Hospital, Shanghai Jiaotong University School of Medicine. The immortalized human gastric mucosal cell line GES-1 and AGS were obtained from the Cell Bank of the Chinese Academy of Sciences (Shanghai, China). Cells were routinely cultured with RPMI-1640 medium supplemented with 10% fetal bovine serum and 1% antibiotics (100 µg/mL streptomycin and 100 units/mL penicillin) at 37°C in an incubator with a 5% CO₂ atmosphere.

Establishment of stable Krt17-silenced cell lines

Short hairpin RNA (ShRNA) sequences targeting Krt17 (Krt17-sh1:5'-GCCAGUACUACAGGACAAUT-3'; Krt-sh2:5'-GGUGCGUACCAUUGUGGAATT-3'; and a negative control sequence (control: 5'-TTCTCCGAACGTGTCACGT-3') were synthesized and transfected into pGLVU6/Puro vector (GenePharma corporation, Shanghai, China). 293T cells were utilized for virus packaging after co-transfection of target plasmids using Lipofectamine 3000 (Invitrogen). Viruses were obtained at 48 h after transfection. The target cells (1×10^5), including SGC7901 and AGS cells, were infected with the filtered lentivirus. The stable Krt17 silenced cells were selected by culturing with 2 $\mu\text{g}/\text{mL}$ puromycin (Sigma-Aldrich) for 2 weeks and the silencing effects were determined by qRT-PCR and western blot analysis.

qRT-PCR

We extracted total cellular mRNA using TRIzol reagent (Takara) and then performed reverse transcription with the PrimeScript RT-PCR kit (Takara) according to the protocol provided. The mRNA expression of Krt17 (sense: 5'-GGTGGGTGGT GAGATCAATGT-3'; anti-sense: 5'-CGCGTTCAGT TCCTCTGTC-3') was determined by real-time PCR using SYBR Premix Ex Taq (Takara) and a 7500 real-time PCR system (Applied Biosystems) at the following cycling settings: one initial cycle at 95°C for 10 s, 40 cycles at 95°C for 5 s, followed by 30 s at 60°C. Data given were normalized to 18s expression (sense: 5'-TGCGAGTACTCAACACCAACA-3'; anti-sense: 5'-GCATATCTTCGGCCCAACA-3') and represent the average of 3 repeated experiments, and were calculated with the $2^{-\Delta\Delta\text{CT}}$ method.

Western blotting

Total protein of cells and tissue were extracted using a total protein extraction buffer (Beyotime, China). Cell lysates were separated by 10% SDS-PAGE gel electrophoresis and transferred to a nitrocellulose membrane. The membranes were blocked with 5% nonfat milk and incubated with the primary antibodies and then incubated with species-specific secondary antibodies. Image J software was used to quantify the results. Antibodies and their corresponding concentrations used were as follows: Krt17 (1:1000, Proteintech, USA), Bcl2 (1:1000, CST, USA), Bax (1:1000, CST, USA), Bcl-xl (1:1000, CST, USA), Cleaved caspase-3 (1:1000, CST, USA), Cyclin D1 (1:1000, Sigma, USA), Cyclin E (1:1000, Sigma, USA), IRDye680 anti-mouse (1:20000, LI-COR) and IRDye800 anti-rabbit (1:10000, LI-COR). β -actin

(1:1000, CST, USA) was used as a control to ensure the equal loading of protein.

Cell viability assay (CCK8 assay)

NC and shKrt17 GC cells were seeded into 96-well plates at a density of 2000-3000 cells per well with 100 μL medium containing 10% serum. Each group contained 5 wells. Cell Counting Kit-8 (CCK-8, Dojindo, Japan) solution (10 μL) was added to each well after 0, 24, 48, 72 and 96h, respectively. Cell viability was measured using a microplate reader (BIO-TEK) at the absorbance of 450 nm. This experiment was repeated twice at each time point.

In vivo tumour xenograft model

Six-week-old male nude (nu/nu) mice (SLAC, Shanghai, China) were injected subcutaneously in the right flank with the stable cell clones of SGC7901 cells at a density of 5×10^6 , infected with SGC7901-NC or SGC7901-sh1 in 100 μL sterilized phosphate-buffered saline for each nude mouse. Each group contained 6 mice, and the tumor weights were measured and recorded. Six weeks later, all mice were sacrificed and their tumors were dissected, fixed with phosphate-buffered neutral formalin, embedded in paraffin and prepared for standard histological examination. Mice were experimented upon and housed according to protocols approved by the East China Normal University Animal Care Commission.

In vitro Migration and Invasion Assays

For the transwell migration assay, 20000 NC and sh-Krt17 GC cells were seeded on the top chamber of each insert with the noncoated membrane (Millicell). Cells were trypsinized and resuspended in medium and 600-800 μL medium supplemented with 10% fetal bovine serum. 24h later any cells remaining in the top chambers or on the upper membrane of the inserts were carefully removed. After fixation and staining in a dye solution containing 0.1% crystal violet and 20% methanol, cells adhering to the lower membrane of the inserts were counted and imaged using an IX71 inverted microscope (Olympus Corp. Tokyo, Japan). We carried out invasion assays by adding 100 μL matrigel (BD Bioscience, Franklin Lakes, NJ) into top chamber of transwell and placed 40000 NC and shKrt17 GC cells onto the matrigel. 24 h later, the transwell invasion assay was terminated and we proceeded with staining.

Wound healing assay

Cells were seeded into 6-well plates and incubated at 37°C in 5% CO₂ for 24 h until they were 80-90% confluent. Wounds were created on these cells with a sterile pipette tip and cells were cultured in the medium without FBS. After wounding (time 0 h) and

24 h, photographs were taken to assess the ability of the cells to migrate into the wound area (original magnification, 100 ×). Experiments were performed in triplicate and repeated at least three times.

Cell cycle and apoptosis analysis

For cell cycle analysis, transfected cells were cultured for 24 h and then collected and fixed in 70% ethanol at 20°C for 24 h. The fixed cells were washed with phosphate-buffered saline twice before staining with 50µg/mL propidium iodide (Kaiji, NanJing, China). Cell-cycle distribution was analysed by flow cytometry (FACSCalibur, Becton Dickinson, MD, USA). For the apoptosis assay, cells were stained with propidium iodide and Annexin V-fluorescein isothiocyanate (BD Pharmingen) in accordance with the manufacturer's instructions. In brief, the cells were collected and stained with 5µL Annexin V-FITC and 5µL PI for 20 min in the dark and then immediately analysed by flow cytometry.

Statistical analysis

Statistical analyses were performed using SPSS version 21.0 (IBM Corporation) and GraphPad Prism5 (San Diego, CA) software. Clinicopathological characteristics were analysed by the chi-square test. Survival curves were evaluated using the Kaplan-Meier method, and analysed by the log-rank test. Cox's proportional hazards modeling of factors potentially related to survival were conducted to calculate hazard ratios (HR). Differences were compared using a two-tailed Student's *t* test. All *P*-values were determined from 2-tailed tests and differences with a *P*-value < 0.05 was considered to be statistically significant.

Results

The expression of Krt17 is upregulated in GC tissues

To evaluate the expression status of Krt17 in human GC tissues, we first analysed the mRNA expression levels of Krt17 in two independent microarray datasets, including the TCGA and ONCOMINE databases. The results revealed that the expression levels of Krt17 were significantly elevated in tumor tissues compared with normal tissues in both independent datasets. (*P* < 0.001, *P* < 0.001), (Fig. 1A-E). We further examined the protein expression levels of Krt17 in 20 pairs of GC and adjacent normal tissues. Consistent with the data from the TCGA and ONCOMINE databases, the protein expression levels of Krt17 in GC tissues was also increased in 70% (14/20) compared to the adjacent normal tissue (Fig. 1F). We then performed an immunohistochemical analysis of a tissue microarray that contained 569 GC

samples and found Krt17 was highly expressed in the 321 (56.41%) of GC samples, and the rest 248 (43.59%) samples showed a low expression level (Fig. 2). The aforementioned results demonstrated that both the mRNA and protein levels of Krt17 were significantly upregulated in GC tissues.

Table 1. Correlations between Krt17 expression and clinical parameters in 569 GC patients.

Clinicopathological variables	Krt17 Expression		<i>P</i>
	low (n=248, 43.6%)	High(n=321, 56.4%)	
Age			
≥65	94(41.59)	132(58.41)	0.49
<65	154(44.90)	189(55.10)	
Lauren type			
Intestinal type	91(50.28)	90(49.72)	0.701
Diffuse type	157(40.46)	231(59.54)	
Gender			
Male	168(43.08)	222(56.92)	0.717
Female	80(44.69)	99(55.31)	
Tumor size (cm)			
<5	150(49.67)	152(50.33)	0.002
≥5	98(36.70)	169(63.30)	
Histological differentiation			
Well	79(49.38)	81(50.62)	0.091
Moderate/Poor	169(41.32)	240(58.68)	
Depth of invasion (T)			
T1	52(68.42)	24(31.58)	<0.001
T2	35(43.75)	45(56.25)	
T3	60(39.74)	91(60.26)	
T4	101(38.55)	161(61.45)	
Lymph node metastasis(N)			
N0	121(56.02)	95(43.98)	<0.001
N1	45(42.86)	60(57.14)	
N2	38(33.33)	76(66.67)	
N3	44(32.84)	90(67.16)	
TNM stage			
I	72(60.50)	47(39.50)	<0.001
II	80(48.48)	85(51.52)	
III	94(33.69)	185(66.31)	
IV	2(33.33)	4(66.67)	
Distant metastasis			
Absent	246(43.69)	317(56.31)	0.701
Present	2(33.33)	4(66.67)	
Vascular invasion			
Negative	217(45.68)	258(54.32)	0.023
Positive	31(32.98)	63(67.02)	
Neural invasion			
Negative	225(45.00)	275(55.00)	0.071
Positive	23(33.33)	46(66.67)	

**P*<0.05 (bold values) are statistically significant

The expression of Krt17 is correlated with clinicopathological features and acts as a poor prognostic factor in patients with GC

In order to obtain a deeper understanding of the clinical significance of Krt17, the chi-square test was used to analyse the association between Krt17 expression and the clinicopathological parameters of patients with GC. We found that Krt17 expression in GC tissues closely correlated with the tumor size (*P* <

0.01), depth of invasion (T) ($P < 0.001$), lymph node metastasis(N) ($P < 0.001$), TNM stage ($P < 0.001$) and vascular invasion ($P < 0.05$). However, no significant difference was detected between Krt17 expression and age or gender (Table 1).

To determine the prognostic value of Krt17 for GC, the relationship between Krt17 expression and the clinical follow-up data was analysed using Kaplan-Meier analysis and the log-rank test. The

results demonstrated that high expression of Krt17 was inversely associated with overall survival (OS) ($n = 569$, $P < 0.001$, Fig. 3A), which indicated that patients with higher Krt17 levels had significantly poorer OS than those with lower Krt17 levels. We also determined that high expression of Krt17 was remarkably associated with poor OS, regardless of TNM stage, lymph node metastasis, neural invasion, and vascular invasion (Fig. 3B-I).

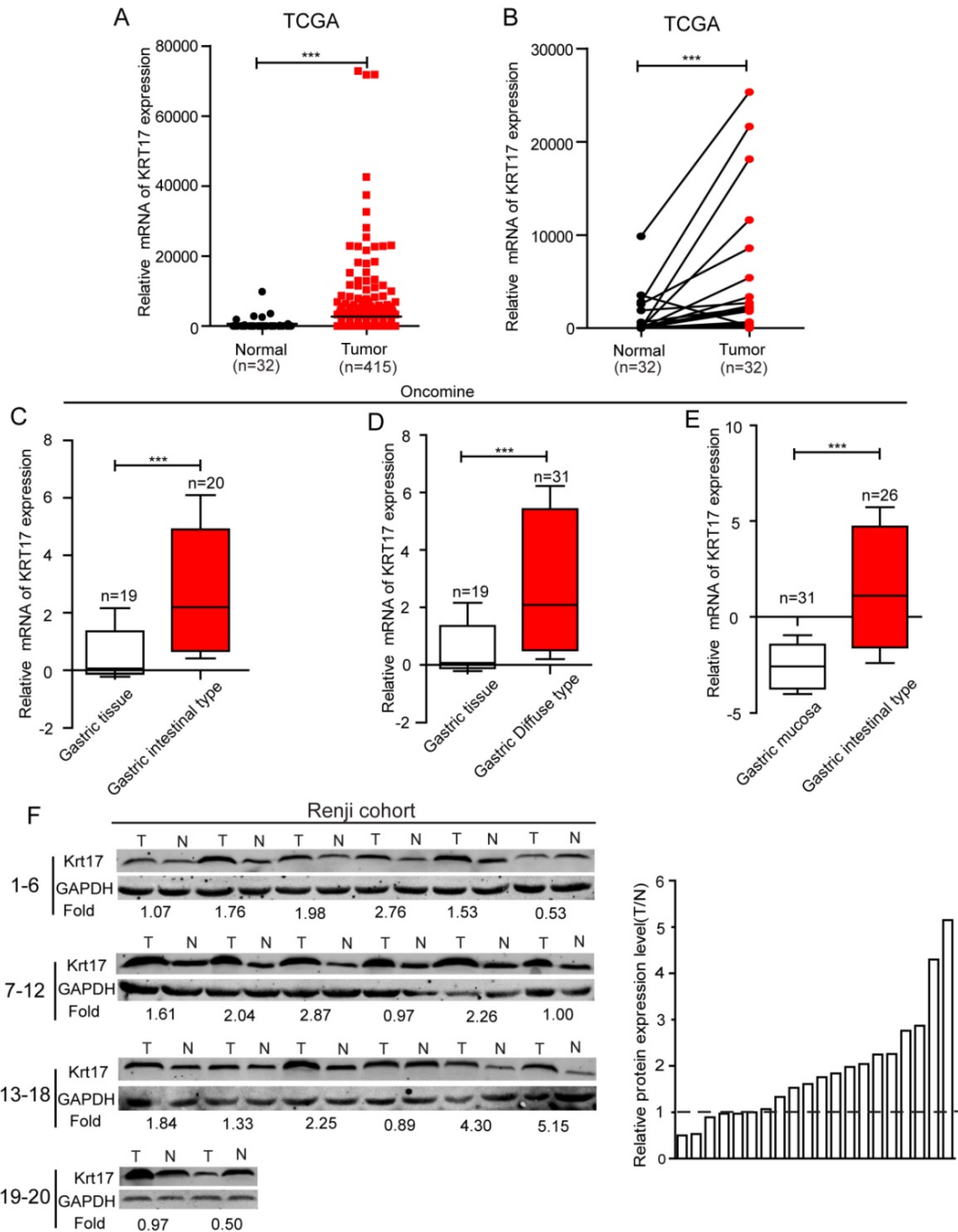


Figure 1. The expression of Krt17 is significantly upregulated in GC tissues. A: The mRNA expression of Krt17 is upregulated in tumor tissues compared with the normal tissues revealed using the TCGA dataset. B: The mRNA expression of Krt17 is upregulated in 32 matched tumor and non-tumor tissue revealed using the TCGA dataset. C: Krt17 is upregulated in GC intestinal type compared with normal gastric tissues. D: Krt17 is increased in GC diffuse type compared with normal gastric tissues. E: Compared with normal gastric mucosa, Krt17 is upregulated in GC intestinal type. F: Krt17 protein expression is elevated in 20 paired GC tissues and normal tissues from Renji hospital via western blotting.

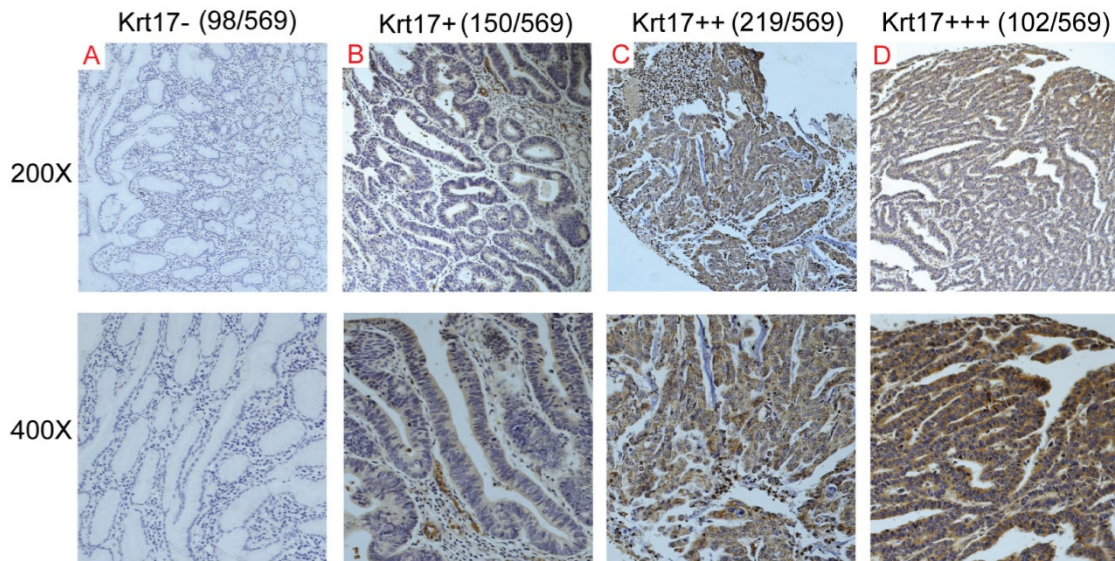


Figure 2. Krt17 expression in GC tissue samples. A-D: Representative images of Krt17 expression in GC are shown at 200x and 400x magnification, respectively. A: GC, scored as (-); B: GC, scored as (+); C: GC, scored as (++); D: GC, scored as (+++).

To directly identify the risk factors associated with OS in patients with GC, univariate and multivariate analyses were performed to confirm whether Krt17 was an independent risk factor for poor prognosis. Univariate Cox regression analyses showed that Lauren type, tumor size, depth of tumor, lymph node metastasis, vascular invasion, neural invasion, expression of Krt17 were significantly associated with OS (Table 2). Furthermore, a multivariate Cox regression analysis identified that tumor size, depth of tumor, lymph node metastasis, vascular invasion, neural invasion, expression of Krt17 were independent predictors of OS in patients with GC (Table 2). Taken together, these data indicated that upregulated expression levels of Krt17 predicted poor prognosis and might contribute to tumor progression in GC.

Silencing of Krt17 suppresses GC cell proliferation *in vitro* and tumor growth *in vivo*

To achieve a better understanding of the biological function of Krt17, we detected Krt17 expression in six GC cell lines using RT-PCR and western blotting. Consistent with the findings in GC tissues, Krt17 expression was upregulated in all six GC cell lines compared with the nonmalignant GES-1 cells (Fig. 4A). Two GC cell lines with relatively higher Krt17 expression (SGC7901 and AGS cells) were selected for loss-of-function analysis. SGC7901 and AGS were transfected with shKrt17 (1, 2), designated as sh1, sh2, and a mock vector, which was marked as NC. The silencing effects of the shRNAs in two cell lines were detected by RT-PCR and western blotting, which showed that Krt17 mRNA and protein

expression levels were both significantly decreased by sh1 and sh2 (Fig. 4B).

To explore the effect of Krt17 on GC cell growth, SGC7901 and AGS cell lines were transfected with sh1 and sh2, and were used to detect cell proliferation using CCK8 assay. The results showed that reducing expression of Krt17 significantly suppressed the proliferation of the SGC7901 and AGS cells *in vitro* ($P < 0.001$) (Fig. 4C-D), and we further confirmed the inhibitory role of silencing Krt17 in GC cells proliferation *in vivo* by subcutaneously inoculating SGC7901-sh2 and NC cells into nude mice. After 30 days, tumors derived from sh2 cells were remarkably smaller than those derived from control cells (Fig. 4E). The average tumor weights and volumes in SGC7901/NC mice were $0.48 \text{ g} \pm 0.06 \text{ g}$ and $0.30 \pm 0.05 \text{ cm}^3$, in contrast to $0.05 \pm 0.03 \text{ g}$ and $0.05 \pm 0.02 \text{ cm}^3$ in SGC7901/sh1 mice ($P < 0.01$) (Fig. 4F). Krt17 expression in the tumors was determined using IHC staining, and the results showed that Krt17 expression levels in SGC7901/sh1 derived tumors was markedly lower than NC derived tumors. Moreover, tumor regression was accompanied with significantly increased expression levels of cleaved caspase3, a key executioner of apoptosis, and reduced expression of the proliferation index, PCNA (Fig. 4G).

Taken together, our data demonstrated that silencing Krt17 in GC cells suppressed cell proliferation *in vitro* and reduced tumorigenicity *in vivo*.

Silencing of Krt17 reduces the migration and invasive capacity of GC cells *in vitro*

In order to determine whether Krt17 influenced

the migration and invasive ability of GC cells, we performed transwell assays and wound healing assays. The results showed knockdown of Krt17 notably blocked the migration and invasion of

SGC7901 and AGS cells compared with the NC (Fig. 5A-I), which indicated that Krt17 promoted a more migratory and invasive phenotype in GC cells.

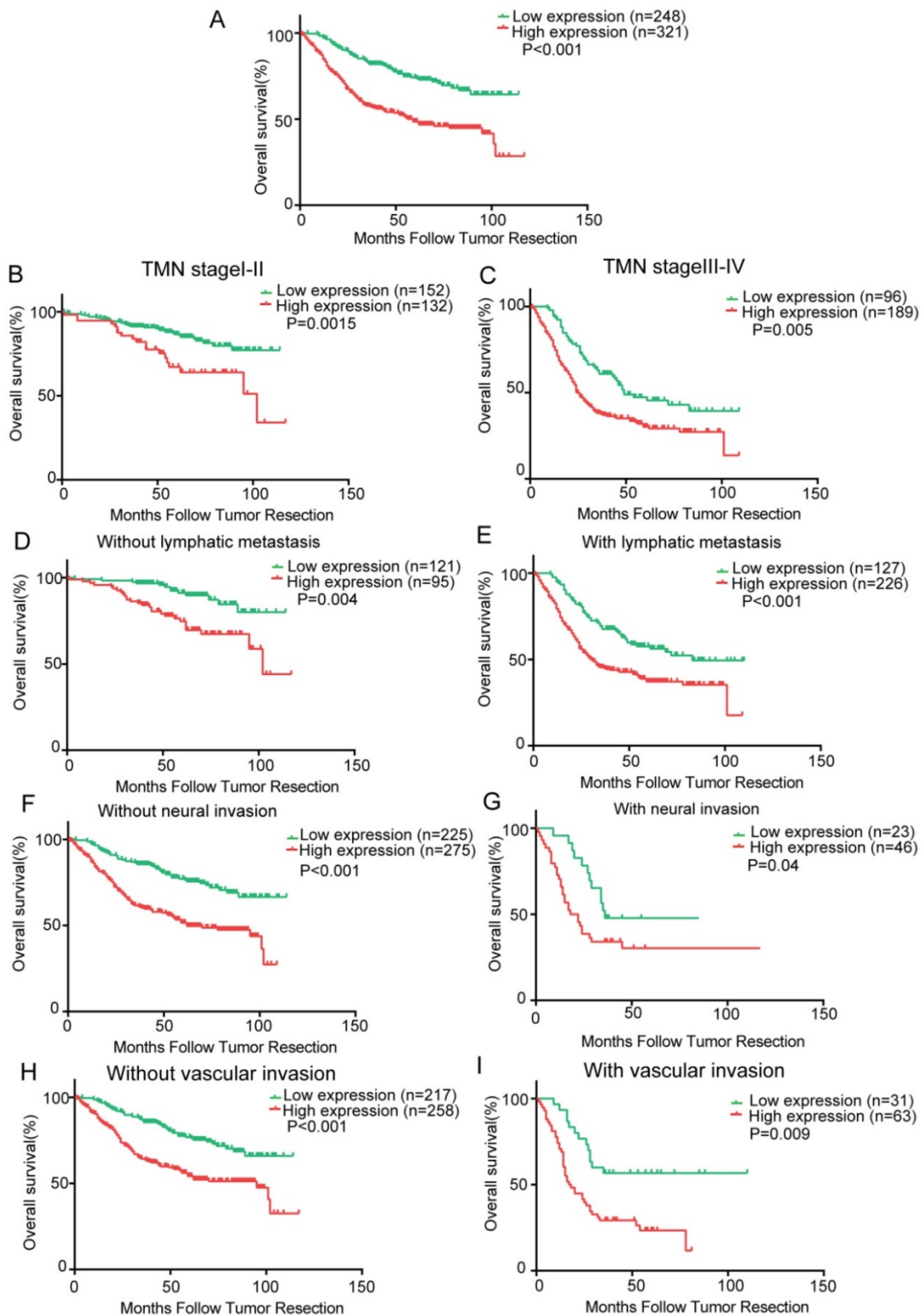


Figure 3. Kaplan-Meier analysis of overall survival in GC patients. A: Krt17 expression is correlated with overall survival in GC patients and high expression level of Krt17 was significantly correlated with poor survival of GC; B-I Correlation between Krt17 expression and overall survival is independent of clinical stage (B-C), lymphatic metastasis (D-E), neural invasion (F-G) and vascular invasion (H-I). P-values were calculated by log-rank test.

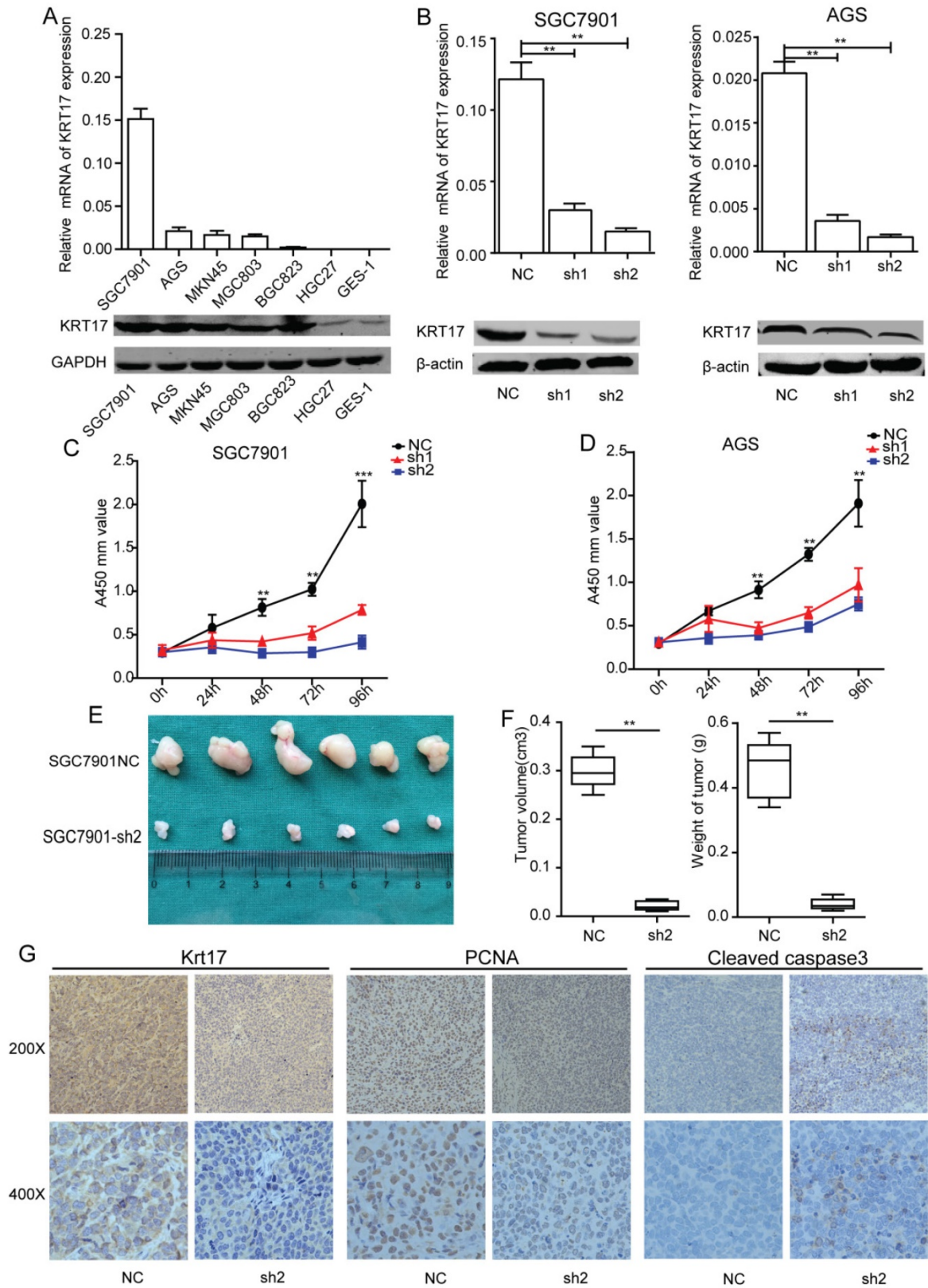
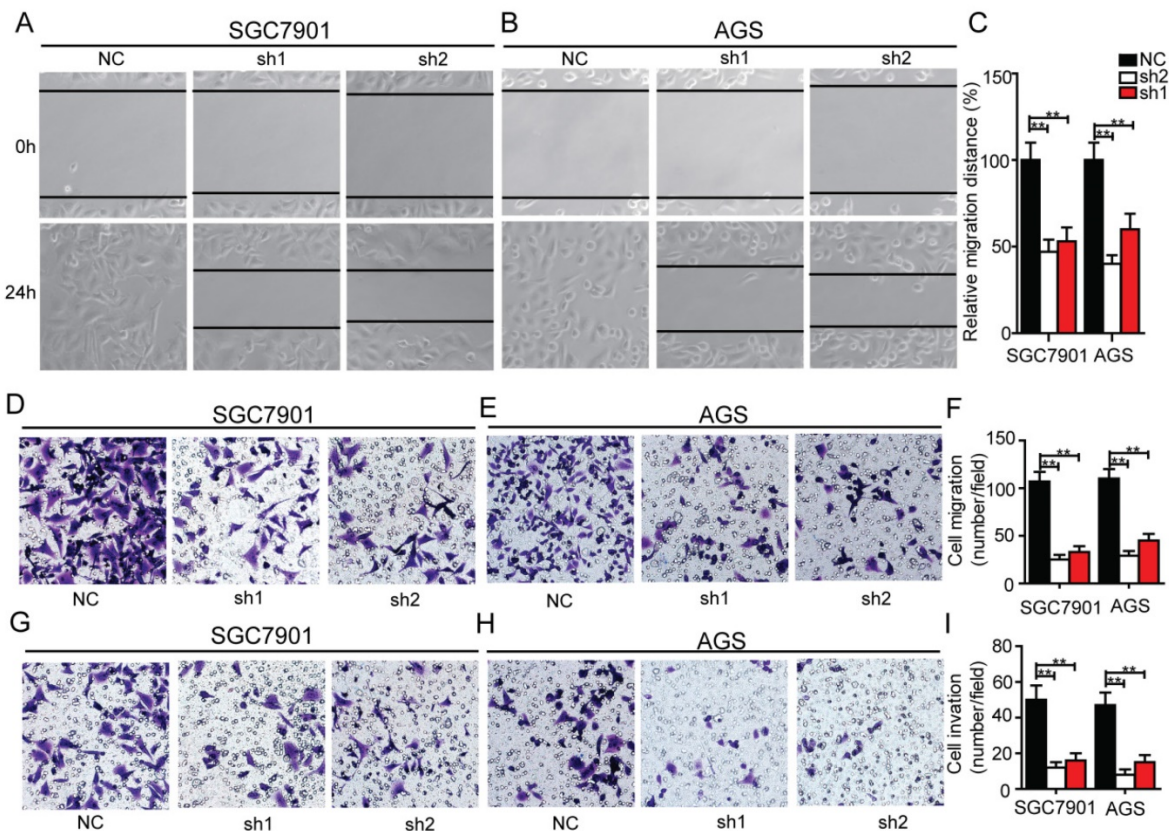


Figure 4. Silencing of Krt17 suppressed gastric cancer cell proliferation *in vitro* and tumor growth *in vivo*. A: qRT-PCR and western blotting showed the Krt17 expression in 7 GC cell lines. B: Krt17 knockdown efficiency was confirmed by qRT-PCR and western blot in SGC7901 and AGS cells. C: The cell proliferation of NC and sh1, sh2 groups in SGC7901 and AGS cells were evaluated by CCK8 assay at 0, 24, 48, 72, 96 h, respectively. D: Photographs of tumors from mice inoculated with SGC7901/NC and SGC7901/sh2 cells. E: Tumor volumes and tumor weights of NC and sh2 groups from D, n = 6. F: Representative images of Krt17, cleaved caspase3 and PCNA in tissues from NC and sh2 mice detected by IHC staining. Compared with NC mice, decreased expression of PCNA and increased expression of cleaved caspase3 were observed in the tissue samples of sh2 (*P < 0.05, **P < 0.01).

Table 2. Univariate and multivariate analysis of prognostic parameters for OS in 569 GC patients by Cox proportional hazards regression.

Prognostic parameter	Univariate analysis			Multivariate analysis		
	HR	95%CI	P	HR	95%CI	P
Age (<65,>=65)	0.856	0.721-1.016	0.075	-	-	-
Gender (male,female)	0.988	0.827-1.180	0.892	-	-	-
Lauren type (Intestinal, Diffuse)	1.215	1.018-1.451	0.031	0.992	0.823-1.196	0.933
Tumor size (<5,>=5cm)	1.598	1.354-1.887	<0.001	1.299	1.071-1.582	0.008
Depth of invasion (T1,T2,T3,T4)	1.105	1.027-1.188	0.008	0.911	0.832-0.998	0.046
Lymph node metastasis (N1,N2,N3,N4)	1.386	1.292-1.487	<0.001	1.299	1.194-1.413	<0.001
Vascular invasion (negative, positive)	2.208	1.763-2.765	<0.001	1.539	1.203-1.970	0.001
Neural invasion (negative, positive)	1.89	1.462-2.443	<0.001	1.579	1.206-2.067	0.001
Distant metastasis (absent,present)	1.632	0.729-3.654	0.234	-	-	-
Expression of krt17 (low, high)	1.454	1.231-1.717	<0.001	1.336	1.128-1.582	0.001

**Figure 5.** Silencing of Krt17 inhibited migration and invasion in GC cell. A-B: Representative wound healing images of SGC7901 and AGS at 0 and 24 h, respectively, the cell boundary was marked by the dotted black line. C: Relative migration distance was analyzed in SGC7901 cells and AGS cells respectively. D-F: Representative migration images of Krt17 silenced and NC cells. G-I Representative invasion images of Krt17 silenced and NC cells. Original magnification: 200 ×. Calculation of cell number were performed with three randomly selected fields. Data are means ± SD (*P < 0.05, **P < 0.01).

Silencing of Krt17 induces apoptosis and cell-cycle arrest at G1/S phase of GC cells

We examined the contribution of apoptosis to the observed growth inhibition of Krt17 silenced cells by using flow cytometry with Annexin V and PI double staining. Krt17-silenced SGC7901 cells (Krt17-Sh1, Krt17-Sh2) acquired a much higher apoptosis ratio compared with SGC7901 cells transfected with NC (Fig. 6A). This phenomenon was also observed in Krt17-silenced AGS cells, where the proportions of both early apoptotic cells and late

apoptotic cells had been significantly increased compared with the control NC-transfected AGS cells (Fig. 6B). The noticeable inhibition of cell proliferation by the knockdown of Krt17 also prompted us to assess the effects of Krt17 on cell-cycle distribution of GC cells, downregulation of Krt17 levels in SGC7901 cells increased the percentage of cells in G1/G0 phase compared with controls and decreased the percentage of cells in S phase (Fig. 6C). The reduction of Krt17 levels in AGS cells decreased the percentage of cells in S phase and increased the percentage of cells in

G1/G0 phase (Fig. 6D). We further examined the expression of apoptosis regulators and several cell-cycle regulators by western blotting, and the results showed that the reduction of Krt17 in both

SGC7901 and AGS cells decreased the levels of cyclin E, cyclin D1, and anti-apoptotic protein Bcl2, while causing increased expression of apoptotic proteins Bax and cleaved caspase-3 (Fig. 6E).

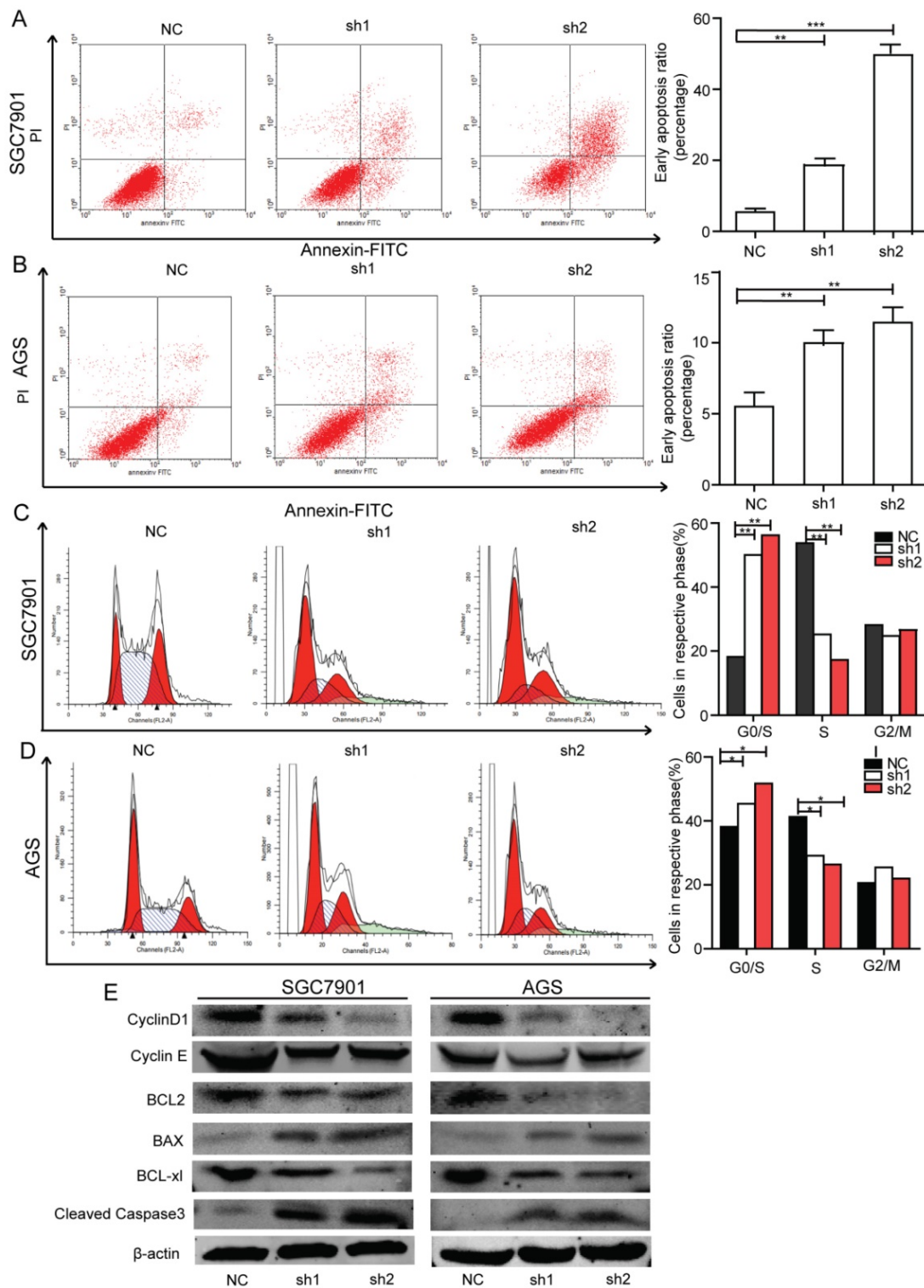


Figure 6. Effect of Krt17 on the cell cycle and apoptosis in GC cells. A-B: Downregulation of Krt17 significantly increased apoptosis in SGC-7901 and AGS cells, the statistical results are shown on the left (*P < 0.05, **P < 0.01). C-D: Silencing of the Krt17 in SGC-7901 and AGS cells decreased cells at G0/G1 phase and increased cells at S phase, the statistical results are shown on the left (*P < 0.05, **P < 0.01). E: Western blot analysis of cell-cycle regulators cyclin E, cyclin D1, the expression of Bcl2, Bax, Bcl-xl and cleaved caspase3 were also determined.

Discussion

Krt17 is a member of type 1 acidic epithelial keratin family, which acts as a promoter of epithelial proliferation, and has been identified as an oncogene, participating in several processes involved in the occurrence of tumors. To date, Krt17 has been reported to be overexpressed in malignant lesions of the cervix, and plays a role in cervical tumorigenesis [22]. Similarly, Krt17 has been found in a poor prognostic phenotype of human colorectal carcinoma [18]. Previous studies reported that Krt17 was frequently expressed in the cytoplasm of tumor cells in patients with GC, and may correlate with tumor progression [23]. However, its exact biological role in GC remains elusive.

The abilities to predict outcome and to identify key players in biological mechanisms that lead to poor outcome are two important objectives in cancer research [24]. In our study, we first analysed GC microarray data from several different databases and found that mRNA expression of Krt17 was significantly upregulated in GC tissues compared to normal tissues. Furthermore, we ascertained that expression of Krt17 in a large panel of GC samples (569 cases) was positively correlated with the TMN stage, lymphatic metastasis, depth of invasion and vascular invasion. Noticeably, Kaplan-Meier survival analysis indicated that patients with high Krt17 expressions level exhibited a remarkable shorter survival duration than those displaying low Krt17 expression levels, indicating that Krt17 may participate in the development of GC.

Krt17 has been regarded to be of great importance in terms of protein synthesis and cell growth, and thus may have an important influence on cell viability and function. An important study demonstrated that Krt17 positively regulated the cell size and growth of keratinocytes by binding to the adapter protein SFN by stimulating the Akt/mTOR pathway [25]. Recently, Krt17 was established to strengthen the migration and invasive capacity of oral cancer cells via inducing epithelial-mesenchymal transition [26]. With regard to the current study, to further elucidate the potential effects of Krt17 in GC cell lines, we established stable Krt17 silencing of an SGC-7901 cell clone and AGS cell clone to perform loss of function experiments. Our results showed that the proliferative capacity of GC cells was significantly decreased in both *in vitro* and *in vivo*, and the migration and invasive capacity declined remarkably after Krt17 was silenced *in vitro*. IHC analysis of subcutaneous tumors indicated that PCNA (proliferation index) expression was reducing after Krt17 was silenced, while cleaved caspase3, an important apoptosis index,

was increased. In conclusion, our data demonstrated that Krt17 could promote the proliferation, migration, and invasion of GC cells.

Apoptosis, or programmed cell death, is thought to be involved in various biological processes during tumor pathogenesis [27]. The imbalance of cell apoptosis and proliferation is a crucial event in the progression of cancer. In our experiments, we discovered that silencing Krt17 greatly triggered apoptosis in both SGC7901 and AGS cell lines, which indicated that Krt17 inhibited apoptosis in human GC. Moreover, we found that silencing of Krt17 induced apoptosis was associated with altering the expression of the Bcl2 family. The Bcl2 family of proteins is a group of upstream regulators of MOMP that includes both pro- and anti-apoptotic components that predominantly mediate the mitochondrial (intrinsic) apoptotic pathway [28, 29]. Apoptotic protein Bax, as well as cleaved caspase-3, were upregulated, and downregulation of the anti-apoptotic proteins Bcl2 and Bcl-xl were determined by western blot analysis.

We then observed that silencing of Krt17 could notably induce cell cycle arrest at G0/G1 phase. Pathological regulation of cell-cycle processes is an essential aspect of cancer cells [30]. The G1/S transition is vital for cell proliferation and its disorder could lead to the carcinogenesis of various human cancers [31]. Our evaluation of potential mechanisms underlying the influences of Krt17 silencing on the suppression of human GC cell proliferation were focused on the expression of cell cycle-related regulators, and we found that cyclin E and cyclin D1, which were reported to promote cell cycle progression through inducing the G1-S phase transition [32], were significantly downregulated with the silencing of Krt17.

In conclusion, our study demonstrated that Krt17 was significantly upregulated in GC tissues, and that Krt17 expression could serve as an independent prognostic factor in patients with GC. Furthermore, our findings suggest that silencing of Krt17 had a suppressive effect on tumorigenesis in GC cell lines and inhibited cell growth both *in vitro* and *in vivo*. Moreover, Krt17 could regulate cell cycle and modulate cell cycle proteins.

Therefore, the current study revealed that Krt17 may act as an oncogene in GC, further studies to clarify the molecular mechanism may facilitate the development of a new candidate for targeted therapy for GC.

Abbreviations

GC: gastric cancer; Krt17: keratin17; qRT-PCR: quantitative real-time polymerase chain reaction;

TNM: Tumor node metastasis; IHC: Immunohistochemistry; OS: Overall survival; ShRNA: Short hairpin RNA; PI: Propidium Iodide.

Acknowledgments

This work was supported by the grant from projects of Science and Technology Commission of Shanghai Municipality (No.15410723000), Shanghai City Committee of Science and Technology Key Project (ZY3-CCCX-3-2003), Shanghai International Technology Cooperation Fund (15410723000), Projects of Science and Technology Commission of Shanghai Municipality (No. 17ZR1416800), Projects of Shanghai Municipal Commission of Health and Family Planning (No.2017BR043) and Projects of Shanghai Hospital Development Center (SHDC12016236).

Ethical standard

The use of samples in this study was permitted by committee of Renji Hospital, Shanghai Jiaotong University School of Medicine. All tissue samples were acquired with the consent of patients according to the standard of the China Ethical Review Committee.

Competing Interests

The authors have declared that no competing interest exists.

References

- [1] Siegel R, Ma J, Zou Z and Jemal A. Cancer statistics, 2014. *CA Cancer J Clin* 2014; 64: 9-29.
- [2] Zhang ZZ, Zhao G, Zhuang C, Shen YY, Zhao WY, Xu J, Wang M, Wang CJ, Tu L, Cao H and Zhang ZG. Long non-coding RNA LINC00628 functions as a gastric cancer suppressor via long-range modulating the expression of cell cycle related genes. *Sci Rep* 2016; 6: 27435.
- [3] Shi Y and Zhou Y. The role of surgery in the treatment of gastric cancer. *J Surg Oncol* 2010; 101: 687-692.
- [4] Coburn NG. Lymph nodes and gastric cancer. *J Surg Oncol* 2009; 99: 199-206.
- [5] Karantza V. Keratins in health and cancer: more than mere epithelial cell markers. *Oncogene* 2011; 30: 127-138.
- [6] Kurokawa I, Takahashi K, Moll I and Moll R. Expression of keratins in cutaneous epithelial tumors and related disorders--distribution and clinical significance. *Exp Dermatol* 2011; 20: 217-228.
- [7] Salas PJ, Forteza R and Mashukova A. Multiple roles for keratin intermediate filaments in the regulation of epithelial barrier function and apico-basal polarity. *Tissue Barriers* 2016; 4: e1178368.
- [8] Papafotiou G, Paraskevopoulou V, Vasilaki E, Kanaki Z, Paschalidis N and Klinakis A. KRT14 marks a subpopulation of bladder basal cells with pivotal role in regeneration and tumorigenesis. *Nat Commun* 2016; 7: 11914.
- [9] Huang B, Song JH, Cheng Y, Abraham JM, Ibrahim S, Sun Z, Ke X and Meltzer SJ. Long non-coding antisense RNA KRT7-AS is activated in gastric cancers and supports cancer cell progression by increasing KRT7 expression. *Oncogene* 2016; 35: 4927-4936.
- [10] Moll R, Franke WW, Volc-Platzter B and Krepler R. Different keratin polypeptides in epidermis and other epithelia of human skin: a specific cytokeratin of molecular weight 46,000 in epithelia of the pilosebaceous tract and basal cell epitheliomas. *J Cell Biol* 1982; 95: 285-295.
- [11] Pan X, Hobbs RP and Coulombe PA. The expanding significance of keratin intermediate filaments in normal and diseased epithelia. *Curr Opin Cell Biol* 2013; 25: 47-56.
- [12] Troyanovsky SM, Guelstein VI, Tchipsysheva TA, Krutovskikh VA and Bannikov GA. Patterns of expression of keratin 17 in human epithelia: dependency on cell position. *J Cell Sci* 1989; 93 (Pt 3): 419-426.
- [13] Troyanovsky SM, Leube RE and Franke WW. Characterization of the human gene encoding cytokeratin 17 and its expression pattern. *Eur J Cell Biol* 1992; 59: 127-137.
- [14] Escobar-Hoyos LF, Shah R, Roa-Pena L, Vanner EA, Najafian N, Banach A, Nielsen E, Al-Khalil R, Akalin A, Talmage D and Shroyer KR. Keratin-17 Promotes p27KIP1 Nuclear Export and Degradation and Offers Potential Prognostic Utility. *Cancer Res* 2015; 75: 3650-3662.
- [15] Depianto D, Kerns ML, Dlugosz AA and Coulombe PA. Keratin 17 promotes epithelial proliferation and tumor growth by polarizing the immune response in skin. *Nat Genet* 2010; 42: 910-914.
- [16] Gorski JJ, James CR, Quinn JE, Stewart GE, Staunton KC, Buckley NE, McDyer FA, Kennedy RD, Wilson RH, Mullan PB and Harkin DP. BRCA1 transcriptionally regulates genes associated with the basal-like phenotype in breast cancer. *Breast Cancer Res Treat* 2010; 122: 721-731.
- [17] Rickman DS, Millon R, De Reynies A, Thomas E, Wasyluk C, Muller D, Abecassis J and Wasyluk B. Prediction of future metastasis and molecular characterization of head and neck squamous-cell carcinoma based on transcriptome and genome analysis by microarrays. *Oncogene* 2008; 27: 6607-6622.
- [18] Kim CY, Jung WY, Lee HJ, Kim HK, Kim A and Shin BK. Proteomic analysis reveals overexpression of moesin and cytokeratin 17 proteins in colorectal carcinoma. *Oncol Rep* 2012; 27: 608-620.
- [19] Bourmet B, Pointreau A, Souque A, Oumouhou N, Muscari F, Lepage B, Senesse P, Barthelet M, Lesavre N, Hammel P, Levy P, Ruszniewski P, Cordelier P and Buscail L. Gene expression signature of advanced pancreatic ductal adenocarcinoma using low density array on endoscopic ultrasound-guided fine needle aspiration samples. *Pancreatol* 2012; 12: 27-34.
- [20] Wang Y and Zheng T. Screening of hub genes and pathways in colorectal cancer with microarray technology. *Pathol Oncol Res* 2014; 20: 611-618.
- [21] Zhang ZZ, Hua R, Zhang JF, Zhao WY, Zhao EH, Tu L, Wang CJ, Cao H and Zhang ZG. TEM7 (PLXDC1), a key prognostic predictor for resectable gastric cancer, promotes cancer cell migration and invasion. *Am J Cancer Res* 2015; 5: 772-781.
- [22] Hobbs RP, Batazzi AS, Han MC and Coulombe PA. Loss of Keratin 17 induces tissue-specific cytokine polarization and cellular differentiation in HPV16-driven cervical tumorigenesis *in vivo*. *Oncogene* 2016; 35: 5653-5662.
- [23] Ide M, Kato T, Ogata K, Mochiki E, Kuwano H and Oyama T. Keratin 17 expression correlates with tumor progression and poor prognosis in gastric adenocarcinoma. *Ann Surg Oncol* 2012; 19: 3506-3514.
- [24] Quan Y, Xu M, Cui P, Ye M, Zhuang B and Min Z. Grainyhead-like 2 Promotes Tumor Growth and is Associated with Poor Prognosis in Colorectal Cancer. *J Cancer* 2015; 6: 342-350.
- [25] Kim S, Wong P and Coulombe PA. A keratin cytoskeletal protein regulates protein synthesis and epithelial cell growth. *Nature* 2006; 441: 362-365.
- [26] Chiang CH, Wu CC, Lee LY, Li YC, Liu HP, Hsu CW, Lu YC, Chang JT and Cheng AJ. Proteomics Analysis Reveals Involvement of Krt17 in Areca Nut-Induced Oral Carcinogenesis. *J Proteome Res* 2016; 15: 2981-2997.
- [27] Fesik SW. Promoting apoptosis as a strategy for cancer drug discovery. *Nat Rev Cancer* 2005; 5: 876-885.
- [28] Delbridge AR, Grabow S, Strasser A and Vaux DL. Thirty years of BCL-2: translating cell death discoveries into novel cancer therapies. *Nat Rev Cancer* 2016; 16: 99-109.
- [29] Rojas-Rivera D and Hetz C. TMBIM protein family: ancestral regulators of cell death. *Oncogene* 2015; 34: 269-280.
- [30] Hanahan D and Weinberg RA. Hallmarks of cancer: the next generation. *Cell* 2011; 144: 646-674.
- [31] Stein GS, van Wijnen AJ, Stein JL, Lian JB, Montecino M, Zaidi SK and Braastad C. An architectural perspective of cell-cycle control at the G1/S phase cell-cycle transition. *J Cell Physiol* 2006; 209: 706-710.
- [32] Sherr CJ and Roberts JM. CDK inhibitors: positive and negative regulators of G1-phase progression. *Genes Dev* 1999; 13: 1501-1512.